The dynamics of vertical coalescence of acoustically levitated droplets

Aditya Vashi[1] · Ajeet Singh Yadav[1] · Nam-Trung Nguyen[1] · Kamalalayam Rajan Sreejith[1]

Abstract

Mobility manipulation of liquid droplets is an important task of digital imicrofluidics. Acoustic levitation has revolutionised the contactless manipulation of liquid droplets for various applications. Acoustic levitation technique can be effectively used to manipulate droplets to obtain their coalescence. This paper reports a unique, versatile, and material-independent approach for the vertical coalescence of the droplets suspended in an acoustic levitator. The acoustic power of the levitator is carefully engineered to obtain vertical coalescence of two liquid droplets. Water, 20% and 40% glycerol–water solutions are used as the working liquids. The results of the experiments revealed three outcomes during the coalescence. The outcomes are analysed and discussed.

Keywords Digital microfluidics · Acoustic levitation · Vertical coalescence · Contactless manipulation

1 Introduction

Digital microfluidics (DMF) is a technology that manipulates discrete droplets ranging from picolitre to microlitre sizes (Choi et al. 2012). DMF technology offers advantages such as minimum reagent use, rapid response, and low contamination. As a result, DMF has found applications in biomedical devices (Sreejith et al. 2021), drug development (Jebrail et al. 2012), food processing (Chou et al. 2015), cell biology (Barbulovic-Nad et al. 2008), and biochemical reactions (Sreejith et al. 2019). Common platforms for DMF include liquid drops, liquid marbles (Aussillous et al. 2001), and core-shell beads (Galogahi et al. 2020). Liquid marbles are small liquid droplets coated with hydrophobic or oleophobic powder, while core-shell beads refer to small particles with a core material surrounded by a distinct outer layer of shell material. DMF involves tasks such as droplet dispensing, moving, merging, mixing, and sorting. Among these tasks, droplet coalescence or merging is the process, where two different droplets come in contact and form a single droplet. Understanding the fundamental aspects of droplet coalescence is crucial due to its application in ink-jet printing (Kim et al. 2011), spray cooling (Estes et al. 1995),

sintering in metallurgy (Bellehumeur et al. 1996), emulsification (Dreher et al. 1999), and understanding cloud and raindrop formation (Kovetz et al. 1969; Berry et al. 1974). Thus, researchers have delved into theories and experiments focusing on impacts between droplets and solid surfaces (Yarin 2006), drop falling on liquid pools (Blanchette and Bigioni 2006), and head-on, lateral, or oblique drop-drop interaction (Jin et al. 2018; Tang, Zhang, and Law 2012).

In the last two to three decades, research on droplet coalescence has been extended to space conditions due to the importance of its unique micro gravity environment (McCraney et al. 2022; Antar etal. 2003; Savino et al. 2003). The lack of gravity in space permits the containment of fluid through surface energy without the need for any contact or containers (Gulati et al. 2017; Vashi at al. 2023a). This possible contactless liquid handling can prevent heterogeneous nucleation and contamination from a container wall (Hasegawa etal. 2019). On the ground, contactless liquid handling can be achieved with the levitation techniques (Foresti et al. 2013b). Levitation techniques involve suspending solid particles or liquid droplets in air without contact. Levitation can be accomplished through acoustic (Brandt 2001), magnetic (Jayawant 1981), optical (Ashkin et al. 1971), electrostatic (Rhim et al. 1999), and aerodynamic (Hennet et al. 2011) forces. Among these techniques, acoustic levitation uses sound waves to levitate any material, including solids, liquids and small living animals independent of material properties (Andrade

✉ Kamalalayam Rajan Sreejith
  s.kamalalayamrajan@griffith.edu.au

1   Queensland Micro and Nanotechnology Centre, Griffith
    University, 170 Kessels Road, Nathan, QLD 4111, Australia

et al. 2018). These versatilities of acoustic levitation have found applications in analytical chemistry (Santesson et al. 2004), material science (Geng et al. 2022), micro-assembly (Shi et al. 2019) as well as in simulating microgravity on earth (Vashi et al. 2023b).

The capability of acoustic levitation harbours significant potential for contactless droplet coalescence for digital microfluidic applications. Several approaches have been realised for contactless droplet coalescence (Foresti et al. 2013a; Watanabe et al. 2018; Hasegawa et al. 2019; Hasegawa et al. 2020). However, most of the approaches required a complex acoustic levitation system and a significant space to carry out droplet coalescence. Moreover, these techniques have achieved lateral droplet coalescence. Recently, Brotton et al. demonstrated head-on coalescence of droplets in a resonant single-axis acoustic levitator by inducing large amplitude axial oscillation (Brotton et al. 2020). However, this experiment was application-specific and did not delve into the dynamics of the coalescence. Moreover, resonant acoustic levitators use an acoustic emitter and reflector to generate standing acoustic wave that requires proper tuning and control to levitate the material (Andrade, Pérez, and Adamowski 2015). This makes the resonant levitator more complex and costly. In addition, they are also sensitive to environmental conditions such as temperature and pressure. Changes in these conditions can disturb the tunning process of the levitator as well as the levitation stability of the droplet. Compared to resonant acoustic levitators, non-resonant levitators utilise acoustic emitters on both sides to generate the standing wave without requiring distance tuning (Andrade, Pérez, and Adamowski 2015). Non-resonant levitators are also not sensitive to environmental conditions. These advantages make non-resonant levitators easy to operate as well as cost-effective. In this study, we experimentally demonstrated and discussed the contactless vertical coalescence of two droplets levitated in the consecutive nodes of a non-resonant acoustic levitator.

2 Materials and methods

2.1 Experimental setup and procedure

Figure 1 illustrates the schematic of the experimental setup. We used a commercially available acoustic levitator "TinyLev" in the experiment (Marzo et al. 2017). Video of the coalescence was recorded at 2000 fps using a high-speed camera (Photon Fastcam SA3) with Nikon micro lens (AF Micro-NIKKOR 60mm f/2.8D). A White LED light source was positioned at the rear side of the levitator to enhance the image quality. Two droplets were precisely levitated at the consecutive nodes of the levitator using a micropipette (Eppendorf Research® plus – 3123000039). The droplet levitated at the upper node is designated as the upper droplet, and the below droplet is designated as the lower droplet.

Figure 2a depicts the electronic circuit used to perform droplet coalescence. Arduino Nano was used to generate a 40 kHz square wave signal. This signal was amplified by the L297N dual H-bridge motor driver and applied to TinyLev. The electronic circuit was powered by a variable DC power supply (Keithley 2200-30-5). A constant voltage of 10 V was maintained to generate constant acoustic power in the levitator. We hypothesize that the removal of the acoustic power for a short duration may lead the upper droplet to fall on the lower droplet if the upper droplet is larger than the lower droplet. A 13 ms turn-off signal was superimposed to the continuous 40 kHz signal using an additional Arduino UNO microcontroller board.

The equilibrium shape of the levitated droplet depends on the surface tension, gravity, and acoustic force (Vashi et al.
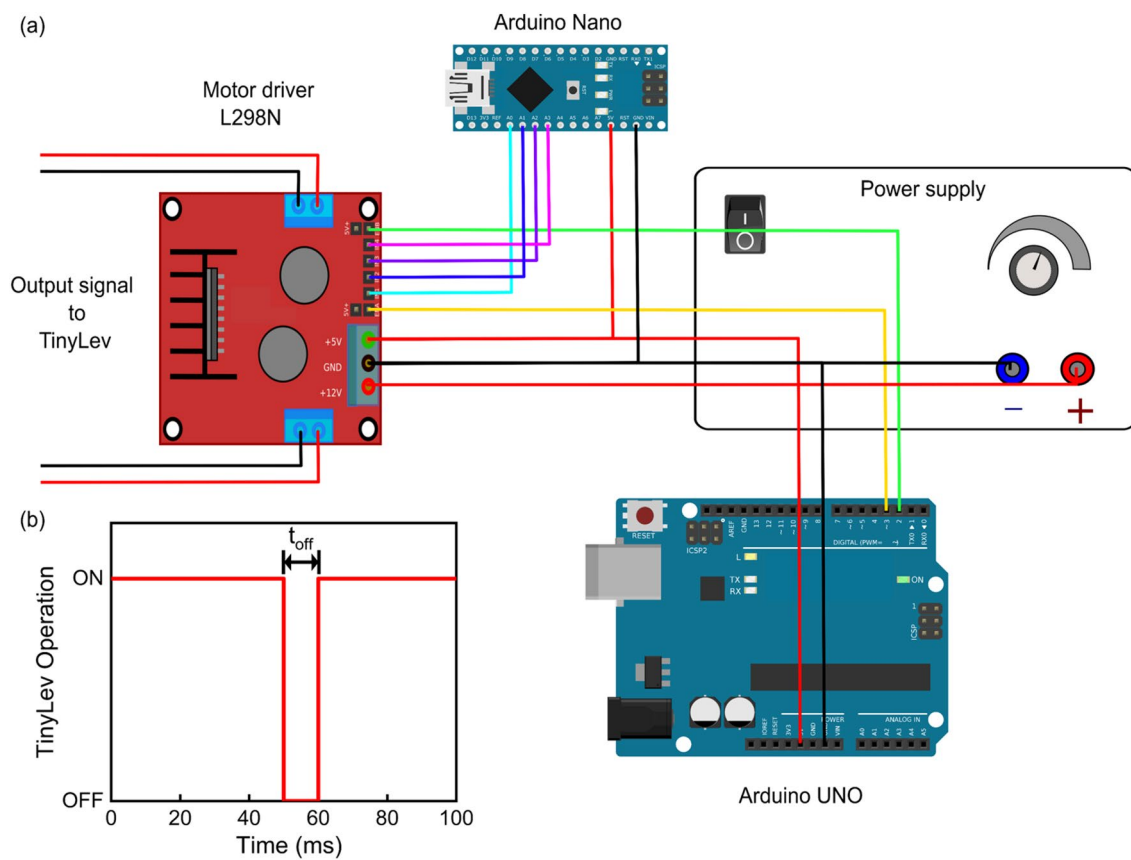
Fig. 1 Experimental setup
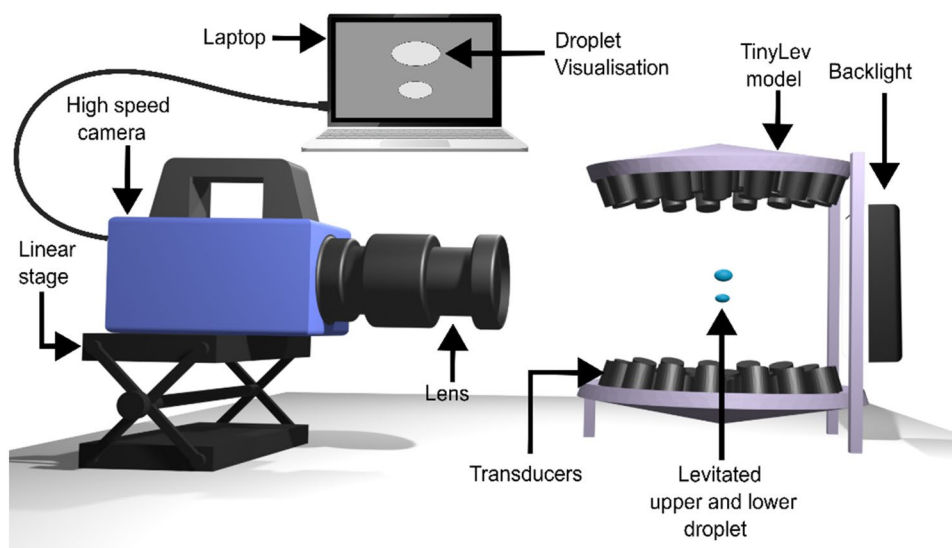
Fig. 2 **a** Electronic driving circuit of TinyLev. **b** Turn off signal for interrupting the acoustic pressure

2023b). As the acoustic power was constant, surface tension and gravity were the factors affecting the stability of droplets in the acoustic cavity. Hence, we used bond number (Bo) to characterize the vertical coalescence. Equation 1 represents the Bond number

$$Bo = \frac{\rho g R^2}{\sigma} \tag{1}$$

where ρ and σ are the density and surface tension of the material, g is the acceleration due to gravity, and R is the radius of the droplet. The main parameters, which drive the head-on coalescence are the surface tension, the viscosity, and the impact velocity (Kumar et al. 2020). Pure deionised water, 20% glycerol–water solution and 40% glycerol–water solution were used as the working liquids. Table 1 shows the

values of density, surface tension and viscosity of the working liquids (Takamura et al. 2012). We kept the bond number of lower droplets the same throughout the experiment for simplicity. Table 2 shows the droplet volumes for various bond numbers. The experiment was repeated 10 times for each combination of lower and upper droplet volumes of the same material.

2.2 Image analysis

We used the bounding rectangle tool of ImageJ to measure the size of droplets. The impact velocity (U) of the droplet is calculated using eq.2.

Material	Density (kg/m^3)	Surface tension (N/m)	Viscosity (Pa s)
Water	998	0.073	0.0010
20% glycerol–water solution	1047	0.071	0.0018
40% glycerol–water solution	1100	0.070	0.0036

Table 1 Properties of working liquids

Table 2 Values of bond number and corresponding volume of working liquids

	Bond number	Volume (μl)		
		Water	20% glycerol–water solution	40% glycerol–water solution
Lower droplet	0.13	4	3.5	3.2
Upper droplet	0.17	6	5.3	4.8
	0.19	7	6.2	5.6
	0.21	8	7.1	6.4
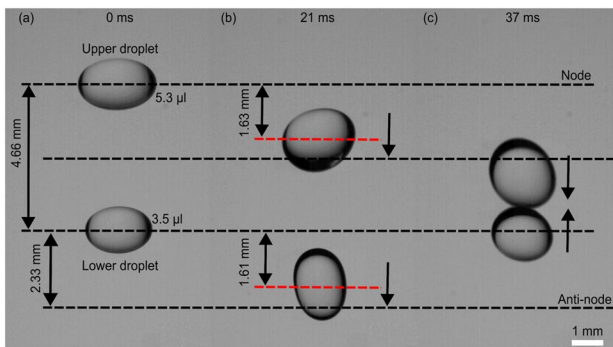
Fig. 3 Various stages of droplet collision. **a** At 0 ms, both droplets are levitated at the corresponding nodes. **b** Following the turnoff signal, from 0 to 21 ms, both droplets descend. **c** Acoustic power was reintroduced between 21 and 37 ms and the upper droplet continues to descend while the lower droplet was pushed back to the original node. At 37 ms the falling upper droplet collide with the lower droplet

$$U = \frac{\sqrt[2]{(x_1 - x_2)^2 + (y_1 - y_2)^2}}{t_1 - t_2} \tag{2}$$

where, (x_1, y_1) is the centroid coordinates of the droplet at impact, (x_2, y_2) is centroid coordinates of droplet 2 frames before impact, and t_1 and t_2 are corresponding times.

3 Results and discussion

3.1 Droplet movement before collision

Figure 3 illustrates the behaviour of both droplets after applying the turn-off signal and before collision. At t = 0 ms, both droplets are stably levitated at consecutive nodes (figure 3a). The distance (d) between two nodes can be calculated as,

$$d = \frac{\lambda}{2} \tag{3}$$

where λ is the wavelength of the ultrasonic waves and can be written as,

$$\lambda = \frac{c}{f} \tag{4}$$

where $c = 343$ m/s is the speed of sound in the air) and $f = 40$ kHz is the frequency of the ultrasonic waves. The theoretical distance between two consecutive nodes was found to be 4.29 mm, closely matching the measured value, of 4.66 mm (Figure 3a). Deactivating the acoustic signal leads to the cessation of acoustic energy within the cavity. Consequently, both droplets initiate a descent under the influence of gravity, Figure 3b. The upper droplet descends by 1.63 mm, while the lower droplet descends by 1.61 mm. These distances correspond to locations characterized by antinode regions, which represent points of maximum acoustic force within the acoustic cavity. Upon reintroducing the acoustic signal, both droplets encounter significantly increased acoustic forces. For the lower droplet, the force stops it from moving down, making it go up to its stable spot at a nodal point, Figure 3c. Conversely, the upper droplet, possessing greater mass due to its larger volume, continues its descent and eventually collides with the lower droplet in the configuration, Figure 3c. The resultant droplet spreads horizontally to the ground plane.

3.2 Characteristic and operation regime of coalescence

The coalescence process led to three possible outcomes: (i) Completely merged droplets, (ii) Partially merged droplets, and (iii) Air core-shell bead (Figure 4). A completely merged outcome indicates the complete coalescence of both droplets without any loss of liquid (Supplementary video 1), while a partially merged outcome involves a coalescence of droplets losing some liquid during the process (Supplementary video 2). The air core-shell bead is the formation of the air core embedded in a liquid shell upon the coalescence (Supplementary video 3). Partially merged droplets and core-shell bead outcomes have resulted from three various phenomena namely the fragmentation (Supplementary video 4), break-up (Supplementary video 2), and buckling (Supplementary video 3).

Fragmentation is the result of atomisation of coalesced droplets after spreading. The generation of high-amplitude capillary waves on the surface of the liquid is the reason for the atomisation (Lee et al. 1991; Yao et al. 2015). This capillary wave can be dampened by increasing the fluid viscosity (Lee et al. 1991). Break-up is the phenomenon, where one daughter droplet is pinched off during the process of coalescence. Fragmentation and breakup resulted in partially merged liquid droplets. In buckling phenomenon, after the spread droplet had formed a curvature and entrapped the air

Fig. 4 Coalescence characteristics for all working liquids
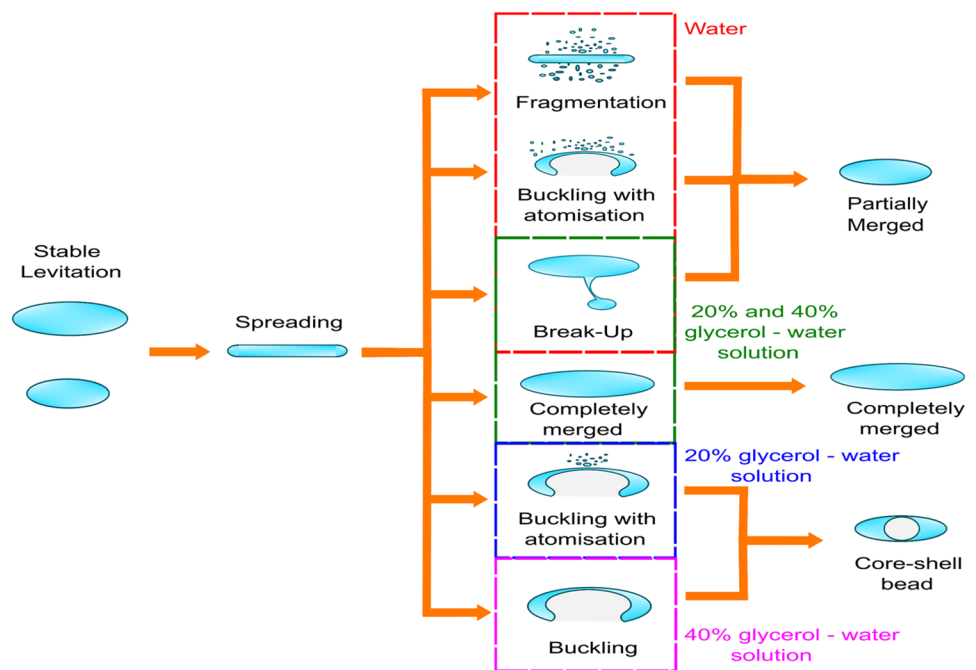
in the curved cavity. The curved geometry of the acoustic levitator is the reason for the buckling (Zang et al. 2018). Once the air volume inside the cavity reaches the critical value, it resonates with the acoustic field and adsorbs sound energy, leading to the rapid closure of the surface entrapping the air inside and forming a core-shell structure with air core and liquid shell (Zang et al. 2018). However, this core-shell structure is still in perturbation until it gets stable at the node position. Moreover, less viscous liquids have less resistance against external forces compared to high viscous liquids due to strong intramolecular forces. Hence, less viscous water shell was unable to keep air core stable and resulted in a partially merged outcome. While higher viscosity of 20% and 40% glycerol–water solutions provides enough resistance to form core-shell bead.

Figure 5a indicates clearly that water droplets coalesced when the levitator was turned off for 14 ms, regardless the Bond numbers. Glycerol–water solutions required a 13 ms turn-off time for coalescence. If the levitator was closed for 12 ms or less, it did not affect the position of either droplet; they remain in place. However, if the levitator was closed for more than 14 ms, both droplets fell. The only outcome for water was partially merged, while glycerol solutions had the potential for all three possible outcomes.

Figures 5b–d illustrate the different outcomes at various Bond numbers for water, 20% glycerol-water solution, and 40% glycerol-water solution, respectively. These results are based on 10 tests. In the case of water, there were 10 partially merged outcomes at bond numbers 0.17, 0.19, and 0.21, respectively. The inset graph provides a detailed breakdown of occurrences at various bond numbers for

water. Buckling happened 9 times and fragmentation happened once for water droplets with a bond number of 0.17. The number of buckling steadily decreases as the bond number increases. The number of buckling for droplets with Bond numbers 0.19 and 0.21 were 7 and 5 respectively. A proportional steady increase in breakup and fragmentation can also be observed as Bond number increases. The number of breakup and fragmentation for droplets with Bond number 0.19 was 1 and 2 respectively. The same for droplets with Bond number 0.21 was 3 and 2 respectively. It is interesting to note that, buckling is the predominant behaviour for merged droplets for all Bond numbers.

For the 20% glycerol-water solution, the completely merged outcome happened 5 times for droplets with a Bond number of 0.17. The number of partially merged and core-shell liquid outcomes were observed 4 and 1 times respectively. Completely merged outcomes were not observed for droplets with Bond numbers 0.19 and 0.21. The number of partially merged and core-shell liquid outcomes were observed 4 and 6 times respectively for droplets with bond number 0.19. The number of partially merged and core-shell liquid outcomes were 5 and 5 for liquid droplets with bond number 0.21.

In the case of the 40% glycerol–water solution, completely merged outcomes occurred 3 times for liquid droplets with a Bond number of 0.17 and 1 for droplets with a Bond number of 0.19. A completely merged outcome was not observed in droplets with Bond number 0.21. Air core-shell liquid outcomes were observed at all the bond numbers with a frequency of 7, 3 and 3 for bond numbers 0.17, 0.19
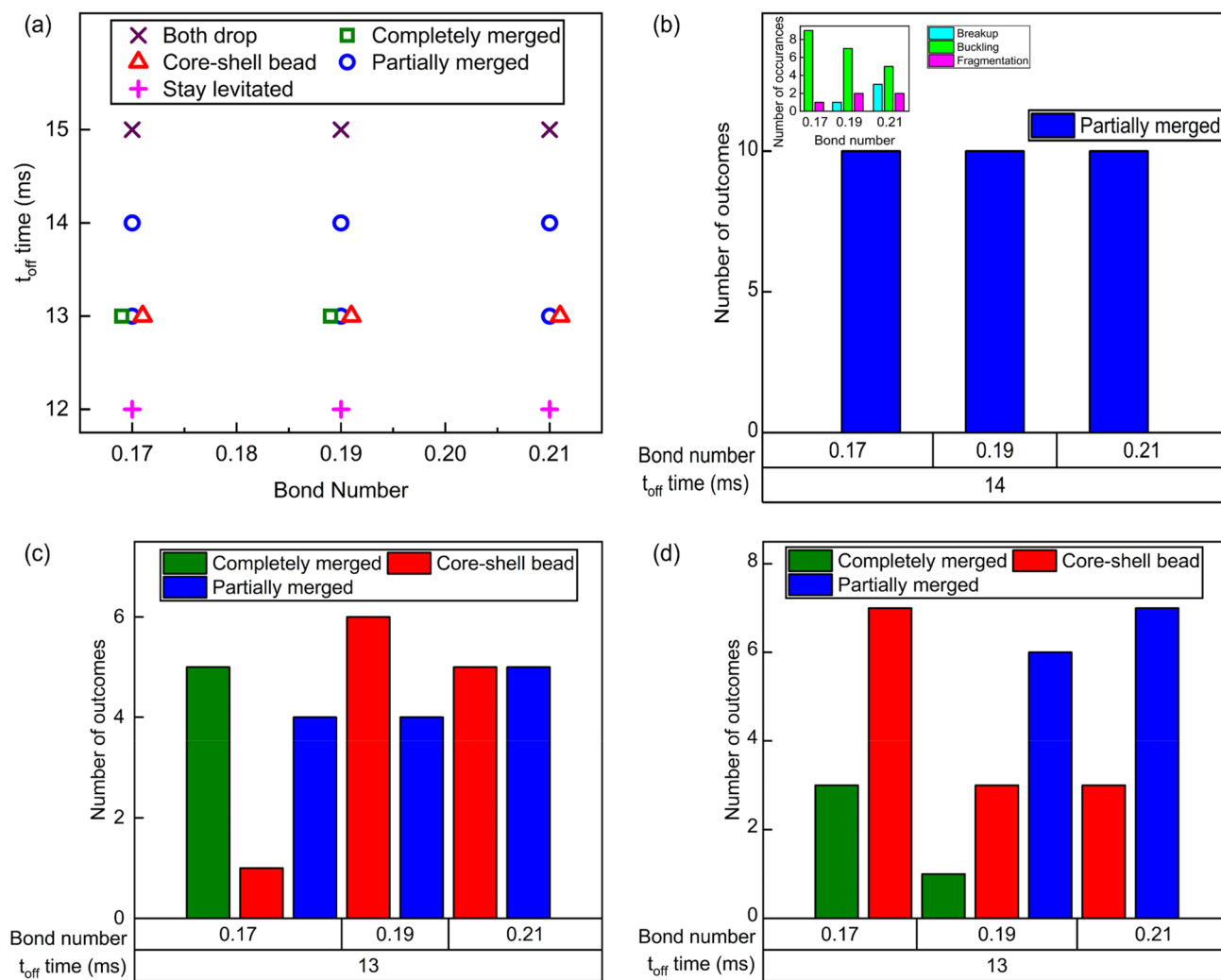
Fig. 5 **a** General operation map of coalescence outcome for different bond number. Number of coalescence outcome for **b** water, **c** 20% glycerol solution, and **d** 40% glycerol solution

and 0.21. The statistics for partially merged outcomes were 6 and 7 for bond numbers 0.19 and 0.21 respectively.

These results indicate that lower Bond numbers are more likely to result in coalescence than higher Bond numbers. However, further investigation is essential to fully understand these variations. The following section provides a characterization of the coalescence process.

3.3 Characterisation of coalescence with spreading

Figure 6 illustrates the relationship between the maximum spreading width of the droplet generated immediately after the collision and various occurrences at different bond numbers for various working liquids. For water, buckling occurred when the spreading width was between 4.75 to 6.0 mm for Bond numbers 0.17 and 0.19, respectively (Fig 6a). For Bond number 0.21, the range of spreading width

was between 5.0 to 5.8 mm to result in buckling. The breakup did not take place for Bond number 0.17. However, for Bond numbers 0.19 and 0.21, a break-up occurred when the spreading width was below 4.5 mm. Low spreading width corresponds to a high thickness of the droplet. The high thickness of the droplet prevents the droplet from bending to form a curve and entraps the air necessary for buckling. Moreover, at low thickness, the generated capillary wave amplitude is not enough to atomise the droplet (Lee et al.1991). In addition, lower viscosity made it unable to keep the entire droplet after spreading and resulted in break up instead of completely merging. Fragmentation occurred in droplets with Bond number 0.17, when the spreading width was above 6mm. However, for liquid droplets with Bond numbers between 0.19 and 0.21, the fragmentation range overlaps the buckling range. This overlap could be attributed to higher air-liquid interface instability caused by
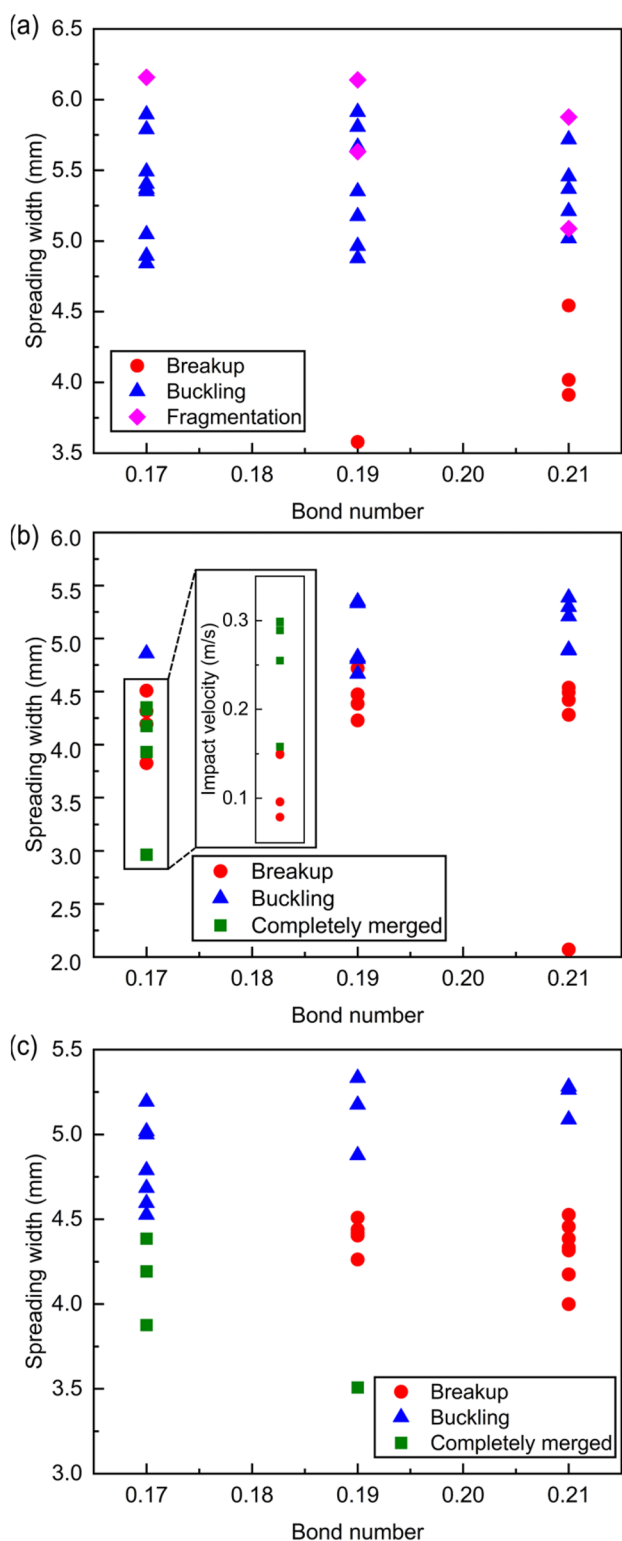
Fig. 6 Variation in maximum spreading width for different bond numbers. **a** Water, **b** 20% glycerol–water solution, **c** 40% glycerol-water solution.

the presence of high-amplitude capillary waves (Lee, Anilkumar et al. 1991). Therefore, droplet atomisation took place before buckling and resulted in fragmentation.

Figure 6b depicts the relationship between the spreading width of coalesced droplets of 20% glycerol-water solution and various occurrences. For bond number 0.17, buckling only occurred at a spreading width of around 4.8 mm. While buckling range for 0.19 and 0.21 bond numbers is between 4.6 and 5.5 mm (Fig 6b). It is interesting to note that below 4.6 mm, breakup and completely merged occurrences overlap for Bond number 0.17 despite having the same bond number and viscosity. Other parameter that could affect the result is the impact velocity. Further investigation shows that upper droplet impact velocity contributes to these different outcome occurrences while having minor differences in spreading width. As shown in Fig 6b, an impact velocity of more than 0.15 m/s resulted in a merged droplet, while a lower impact velocity resulted in a breakup. Higher impact velocity provides enough kinetic energy to overcome cohesive force surface tension. As a result, after spreading and during recoiling droplet stayed intact instead of breaking. However, similar to water, spreading width below 4.5 mm resulted in a break up for Bond numbers of 0.19 and 0.21. This result implies that increasing the viscosity from 0.0010 to 0.0018 Pas also not able to hold the droplet completely, leading to partially merged output after the breakup.

Buckling took place for 40% glycerol–water at a spreading width between 4.6 and 5.5 mm (Fig 6c). Interestingly, spreading width below 4.5 mm resulted in completely merged droplets at Bond number of 0.17. The result shows the domination of viscosity in comparison to other parameters during coalescence. For Bond number of 0.19, break up occurred between 4 and 4.5 mm and a completely merged outcome for a spreading width of 3.5 mm. Less spreading helped the droplet to stay intact during coalescence, while others resulted in breakup. At a Bond number of 0.21, all outcomes are breakup below a spreading width of 4.5 mm like water and 20% glycerol-water solution. This indicates that increasing the viscosity has no significant effect during coalescence for high Bond numbers.

The above findings underscore the significance of the maximum spreading width as a crucial parameter influencing the coalescence outcome. Variations in spreading width led to diverse outcomes even for the same Bond number. Remarkably, spreading widths above 4.6 mm and below 6 mm consistently resulted in buckling, revealing an intriguing pattern for generating air core-shell bead outcomes in highly viscous liquids under acoustic levitation. Moreover, with spreading width below 4.5 mm, droplets tend to partially merge or completely merge depending on viscosity and Bond number. At Bond number of 0.17 for 20% glycerol-water solution, we achieved both partially and completely merged outcomes below 4.5 mm spreading width. The above

results emphasise that achieving a completely merged outcome depends on several factors. Moreover, coalescence took place in the presence of acoustic energy. Hence, the droplet experiences non-linear phenomena including acoustic radiation force (Bruus 2012) and acoustic streaming (Sadhal 2012). The effects of these non-linear phenomena on the droplet during coalescence are still unknown. These aspects could be explored further as a potential area for future works.

4 Conclusion

In this paper, we experimentally demonstrated the coalescence of acoustically levitated droplets. We accomplished coalescence by turning off the levitator for a short duration. The coalescence dynamics of droplets in mid-air were investigated experimentally for various liquids. Coalescence occurred for water when the levitator was turned off for 14 ms for all bond numbers 0.17, 0.18 and 0.19. For 20% and 40% glycerol–water solution, the turn-off time was 13 ms for all bond numbers. The coalescence results revealed three different outcomes, namely completely merging, the partially merging and core-shell air bubble. We found that variation in the spreading width after collision and upper droplet impact velocity are the major parameters influencing the outcome of coalescence. Liquid with higher viscosity and spreading width of more than 4.6 mm resulted in air core-shell bead which is a promising digital microfluidic platform (Yadav et al. 2023). Higher viscosity, less spreading width as well as higher impact velocity are required to achieve complete coalescence. Therefore, further investigation is required to explore the optimum combination of liquid properties for droplet coalescence. Insights into contactless droplet coalescence via acoustic levitation gained in this work provide better understanding and design consideration for potential digital microfluidic applications.

Declarations

References

Andrade M AB, Pérez N, Adamowski J C (2015) Particle manipulation by a non resonant acoustic levitator. App Phys Lett 106:1

Andrade M A. B, Pérez N, Adamowski J C (2018) Review of progress in acoustic levitation. Brazilian J Phys 48:190–213

Antar B N, Ethridge E C, Maxwell D (2003) Viscosity measurement using drop coalescence in microgravity. Microgravity-Sci Technol 14:9–19

Ashkin A, Dziedzic JM (1971) Optical levitation by radiation pressure. Appl Phys Lett 19:283–85

Aussillous P, Quéré D (2001) Liquid marbles. Nature 411:924–27

Barbulovic-Nad I, Yang H, Park P S, Wheeler A R (2008) Digital microfluidics for cell-based assays. Lab on a Chip 8:519–26

Bellehumeur C T, Bisaria MK, Vlachopoulos John (1996) An experimental study and model assessment of polymer sintering. Polym Eng Sci 36:2198–207

Berry E X, Reinhardt R L (1974) An analysis of cloud drop growth by collection: part I double distributions. J Atmos Sci 31:1814–24

Blanchette F, Bigioni T P (2006) Partial coalescence of drops at liquid interfaces. Nat Phys 2:254–57

Brandt EH (2001) Suspended by sound. Nature 413:474–75

Brotton Stephen J, Kaiser Ralf I (2020) Controlled chemistry via contactless manipulation and merging of droplets in an acoustic levitator. Anal Chem 92:8371–77

Bruus Henrik (2012) Acoustofluidics 7: the acoustic radiation force on small particles. Lab on a Chip 12:1014–21

Choi K, Ng A HC, Fobel R, Wheeler A R (2012) Digital microfluidics. Annu Rev Anal Chem 5:413–40

Chou W-L, Lee P-Y, Yang C-L, Huang W-Y, Lin Y-S (2015) Recent advances in applications of droplet microfluidics. Micromachines 6:1249–71

Dreher TM, Glass J, O'Connor AJ, Stevens GW (1999) Effect of rheology on coalescence rates and emulsion stability. AIChE Journal 45:1182–90

Estes K A, Mudawar I (1995) Correlation of Sauter mean diameter and critical heat flux for spray cooling of small surfaces. Int J Heat Mass Transf 38:2985–96

Foresti D, Nabavi M, Klingauf M, Ferrari A, Poulikakos D (2013a) Acoustophoretic contactless transport and handling of matter in air. Proc Natl Acad Sci 110:12549–54

Foresti D, Sambatakakis G, Bottan S, Poulikakos D (2013b) Morphing surfaces enable acoustophoretic contactless transport of ultrahigh-density matter in air. Sci Rep 3:3176. https://doi.org/10.1038/srep03176

Galogahi F M, Zhu Y, An H, Nguyen N-T (2020) Core-shell microparticles: generation approaches and applications. J Sci: Advanced Mater Devices 5:417–35

Geng D, Yan N, Xie W, Lü Y, Wei B (2022) Extraordinary Solidification mechanism of liquid alloys under acoustic levitation state. Adv Mater 35:2206464

Gulati S, Raghunandan A, Rasheed F, McBride S A, Hirsa A H (2017) Ring-sheared drop (RSD): microgravity module for containerless flow studies. Microgravity Sc Technol 29:81–89

Hasegawa K, Watanabe A, Abe Y (2019) Acoustic manipulation of droplets under reduced gravity. Sci Rep 9:16603

Hasegawa K, Watanabe A, Kaneko A, Abe Y (2020) Coalescence dynamics of acoustically levitated droplets. Micromachines 11:343

Hennet L, Cristiglio V, Kozaily J, Pozdnyakova I, Fischer HE, Bytchkov A, Drewitt J W E, Leydier M, Thiaudière D, Gruner S (2011) Aerodynamic levitation and laser heating. The Eur Phys J Spec Topics 196:151–65

Jayawant B V (1981) Electromagnetic levitation and suspension techniques. Rep progress in phys 44(4):411–477

Jebrail Mais J, Bartsch Michael S, Patel Kamlesh D (2012) Digital microfluidics: a versatile tool for applications in chemistry, biology and medicine. Lab on a Chip 12:2452–63

Jin J, Ooi C H, Dao D V, Nguyen N-T (2018) Liquid marble coalescence via vertical collision. Soft Matter 14:4160–68

Kim Y-H, Yoo B w, Anthony J E, Park S K (2011) Controlled deposition of a high-performance small-molecule organic single-crystal transistor array by direct ink-jet printing. Adv Mater 24:497–502

Kovetz A, Olund B (1969) The effect of coalescence and condensation on rain formation in a cloud of finite vertical extent. J Atmos Sci 26:1060–65

Kumar M, Bhardwaj R, Sahu K C (2020) Coalescence dynamics of a droplet on a sessile droplet. Phys Fluids 32:1

Lee CP, Anilkumar AV, Wang TG (1991) Static shape and instability of an acoustically levitated liquid drop. Phys Fluids A: Fluid Dyn 3:2497–515

Marzo Asier, Barnes Adrian, Drinkwater Bruce W (2017) TinyLev: a multi-emitter single-axis acoustic levitator. Rev Sci Instrum 88:085105

McCraney J, Ludwicki J, Joshua Bostwick S, Daniel, Steen P (2022) Coalescence-induced droplet spreading Experiments aboard the International Space Station. Phys Fluids 34:12

Rhim W-K, Ohsaka K, Paradis P-F, Erik R, Spjut (1999) Noncontact technique for measuring surface tension and viscosity of molten materials using high temperature electrostatic levitation. Rev Sci Instrum 70:2796–801

Sadhal SS (2012) Acoustofluidics 13: analysis of acoustic streaming by perturbation methods. Lab on a Chip 12:2292–300

Santesson S, Nilsson S (2004) Airborne chemistry: acoustic levitation in chemical analysis. Anal Bioanal Chem 378:1704–09

Savino R, Nota F, Fico S (2003) Wetting and coalescence prevention of drops in a liquid matrix. Gr Parabolic Flight Results Micro-Sci Technol 14:3–12

Shi Q, Di W, Dong D, Yap L W, Li L, Zang D, Cheng W (2019) A general approach to free-standing nanoassemblies via acoustic levitation self-assembly. ACS Nano 13:5243–50

Sreejith K R, Gorgannezhad L, Jin J, Ooi C H, Stratton H, Dao D V, Nguyen N-T (2019) Liquid marbles as biochemical reactors for the polymerase chain reaction. Lab on a Chip 19:3220–27

Sreejith K R, Umer M, Dirr L, Bailly B, Guillon P, von Itzstein M, Soda N, Kasetsirikul S, Shiddiky M JA, Nguyen N-T (2021) A portable device for LAMP based detection of SARS-CoV-2. Micromachines 12:1151

Takamura K, Fischer H, Morrow N R (2012) Physical properties of aqueous glycerol solutions. J Petrol Sci Eng 98:50–60

Tang C, Zhang P, Law C K (2012) Bouncing, coalescence, and separation in head-on collision of unequal size droplets. Phys Fluids 24:2

Vashi A, Sreejith KR, Nguyen N (2023a) Lab-on-a-chip technologies for microgravity simulation and space applications. Micromachines 14(1):116. https://doi.org/10.3390/mi14010116

Vashi A, Yadav A S, Nguyen N-T, Sreejith K R (2023b) Parametric analysis of acoustically levitated droplet for potential microgravity application. Appl Acoust 213:109624

Watanabe A, Hasegawa K, Abe Y (2018) Contactless fluid manipulation in air: droplet coalescence and active mixing by acoustic levitation. Sci Rep 8:10221

Yadav A S, Tran D T, Teo A JT, Dai Y, Galogahi F M, Ooi C H, Nguyen N-T (2023) Core–shell particles: from fabrication methods to diverse manipulation techniques. Micromachines 14:497

Yao L, Xuecheng W, Yingchun W, Yang J, Gao X, Chen L, Gréhan G, Cen K (2015) Characterization of atomization and breakup of acoustically levitated drops with digital holography. Appl Opt 54:A23–A31

Yarin AL (2006) DROP IMPACT DYNAMICS: splashing, spreading, receding, bouncing. Annu Rev Fluid Mech 38:159–92

Zang D, Li L, Di W, Zhang Z, Ding C, Chen Z, Shen W, Binks B P, Geng X (2018) Inducing drop to bubble transformation via resonance in ultrasound. Nat Commun 9:3546